

Analysing Gas-Liquid Flow in PEM Electrolyser Micro-Channels

S. S. Lafmejani, A. C. Olesen, S. K. Kær

Energy Technology Department, Aalborg University, Aalborg 9000, Denmark.

PEM water electrolysis is a key component for closing the loop of the renewable energy eco-system. In particular, these high response water electrolyzers are suitable for fluctuating power sources. Conventional PEM water electrolyzers are typically operated at a current density of around 1 A/cm^2 and are fairly expensive. One means of increasing the hydrogen yield to cost ratio of such systems, is to increase the operating current density. However, at high current densities, management of heat and mass transfer in the anode current collector and channel becomes crucial. This entails that further understanding of the gas-liquid flow in both the porous media and the channel is necessary for insuring proper oxygen, water and heat management of the electrolysis cell. In this work, the patterns of vertical upward gas-liquid flow in a $5 \times 1 \times 94 \text{ mm}$ micro-channel are experimentally analysed. A sheet of titanium felt is used as a permeable wall for permeation of air through a column of water similar to the phenomenon encountered at the anode. The transparent setup is operated ex-situ and the gas-liquid flow regimes are identified using a camera.

Introduction

Human caused emission of greenhouse gases (GHG), mostly by the use of fossil fuels for energy production and transportation, is a widely agreed cause of recent climate change (1). In many ways, Denmark has started a green transition. In 2012 an energy agreement was signed, resulting in a target by 2020 where at least 50% of the electricity consumption is to be supplied by wind power, and more than 35% of the total energy consumption to be supplied from renewable energy sources (2). In order to achieve these targets, the full reorganization of the energy matrix with renewable sources will require a high degree of energy availability and storage capacity of secondary fuels from electricity, for the usage in the industry and transport sector. Water electrolysis will play a key role in the future renewable energy system to facilitate storage of intermittent renewable energy from wind and sun. The excess power could be peak-shaved using rapid response PEM electrolysis and generate high pressure (some up to 350 bars (3)), high quality hydrogen. It has also advantages such as high current density, thin membrane, low gas crossover rate, quick response to the power input and that it covers the full nominal power density range (10-100%) (4).

The key challenge facing the hydrogen based energy economy is sustainable production of hydrogen, without dependence on fossil fuels, in large quantities at lower costs than existing technologies. One means of increasing the hydrogen yield to cost ratio

of such systems, is to increase the operating current density. However, at high current densities (higher than 1 A/cm^2), management of heat and mass transfer in the anode current collector and channel becomes crucial and can lead to hot spots.

There are some few experimental studies about two-phase flow in the context of PEM water electrolysis. Selamet et al. (5) visualised two-phase transport in both Anode and Cathode sides of an electrolyser cell by simultaneous neutron radiography and optical imaging. They investigated effects of operating parameters such as current density, temperature and water flow rate on the two-phase distribution. They detected higher water accumulation in the cathode chamber at higher current density. Dedigama et al. (6) used electrochemical impedance spectroscopy (EIS) on a transparent PEM electrolysis cell to provide information about individual contributions to the total impedance (losses) of an electrochemical system such as electrolyte conductivity and electrode processes. Dedigama et al. (7) in another study, simultaneously investigated localised current density mapping and flow visualisation in PEM water electrolysis. They revealed that the current density increases towards the end of the anode channel. Meanwhile, the gas-liquid flow transforms from bubbly to slug flow that fill the channel.

PEM water electrolysis process is very complicated. To understand the influence of each parameter, it makes sense to separate the involved processes. In this context, removing the complexity of electrochemistry will improve the control of influencing parameters. For instance, Yang et al. (8) characterised air-water flow in a miniature square channel (hydraulic diameter of 5 mm) with a gas permeable sidewall (made of a long porous lime wood block) like the two-phase flow is encountered in direct feed methanol fuel cells. They visualized flow patterns in vertical and horizontal flows and identified two-phase flow regimes such as bubbly flow, plug flow, slug flow and annular flow. Meanwhile, they did not find stratified flow in the horizontal flow. They showed that in the vertical flow, a single layer of gas bubble adjacent to the permeable sidewall is formed. They concluded that the annular flow should be avoided in direct methanol fuel cells by simply increasing liquid volumetric flux.

Ito et al. (9) investigated the influence of pore structural properties of current collectors on the performance of PEM electrolyser. They found that current collectors with pore diameters less than $50 \mu\text{m}$ reduce the influence of a decrease in water supply on the membrane resistance. It also enhances the uniform and sufficient contact between current collector and the electrode that results also in reducing activation overpotential.

Management of heat and fluid flow through the micro-channels play a great role in the capability of PEM water electrolysis when working at high current densities. Despite, many studies have been done on gas-liquid flows; still there is a lack of research on gas-liquid flows in micro-sized channels (hydraulic diameter of 1 mm) of PEM water electrolysis. Precisely controlling all the parameters that affect the gas-liquid flow in a PEM water electrolysis cell is quite challenging, hence a simplified setup is constructed consisting of only a transparent channel with a sheet of titanium felt as a permeable wall. Air is then allowed to flow through the porous medium and mix with the liquid water flow along the channel length similarly to the study by Yang et al. (8) conducted for direct methanol fuel cells.

Experimental Equipment

Test section

As illustrated in Figure 1, the test section consisted of a square channel (5mm width by 1mm depth in cross-section area and 94 mm in length) with one of its sidewalls permeable to gases. Water was fed using a small power controlled centrifugal water pump into the test section from the inlet, while the laboratory air in which was decompressed by a regulator was fed into the multiphase flow channel along the porous sidewall. The test setup was made of transparent Plexiglas for visualisation. The permeable wall is a layer of 0.35 mm Titanium felt with the size of 94 mm x 10 mm.

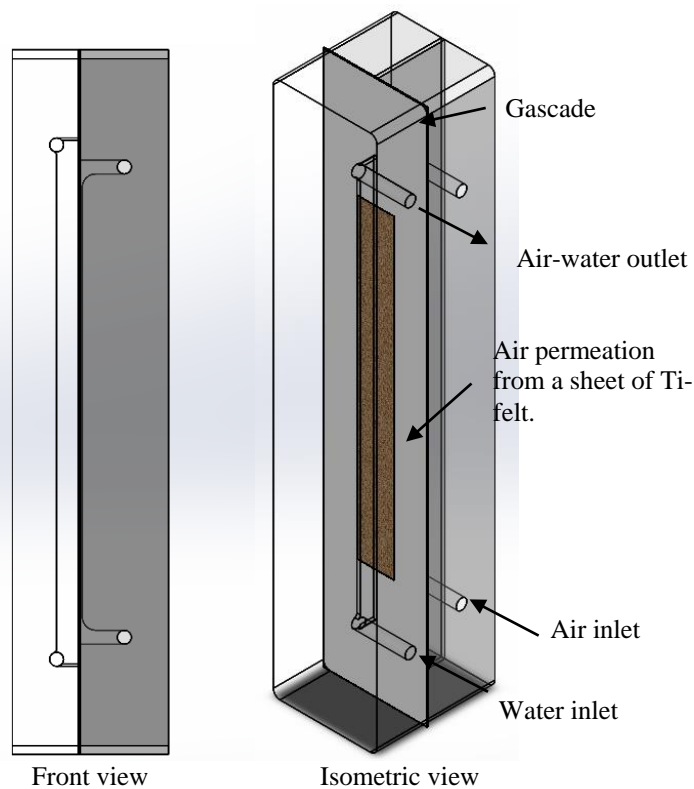


Figure 1: 3D view of the constructed transparent case.

Test setup

Experiments were carried out in the test setup that is schematically shown in Figure 2. DI-Water, pumped from a water tank, passed through a valve, a variable area flow meter, the test section, and eventually returned to the water tank. Simultaneously, the laboratory compressed air was passed through a pressure regulator, a valve, a flow meter and penetrated through the porous sidewall to the test channel from the air channel.

Flow visualization

A Basler acA1300-30um USB 3.0 camera with a Sony ICX445 CCD sensor was employed to visualise flow pattern in the test section with a shoot speed of 30 frames per second at 1.3 megapixel resolution. A Pentax lens with the focal length of 12 mm and the f-stop of 1.2 were used to capture the whole length of the channel at once. A 10 W LED was used to meet the required lightning for capturing images. As shown in Figure 2, the reflected LED light from the wall brights up the gas-liquid flow within the channel.

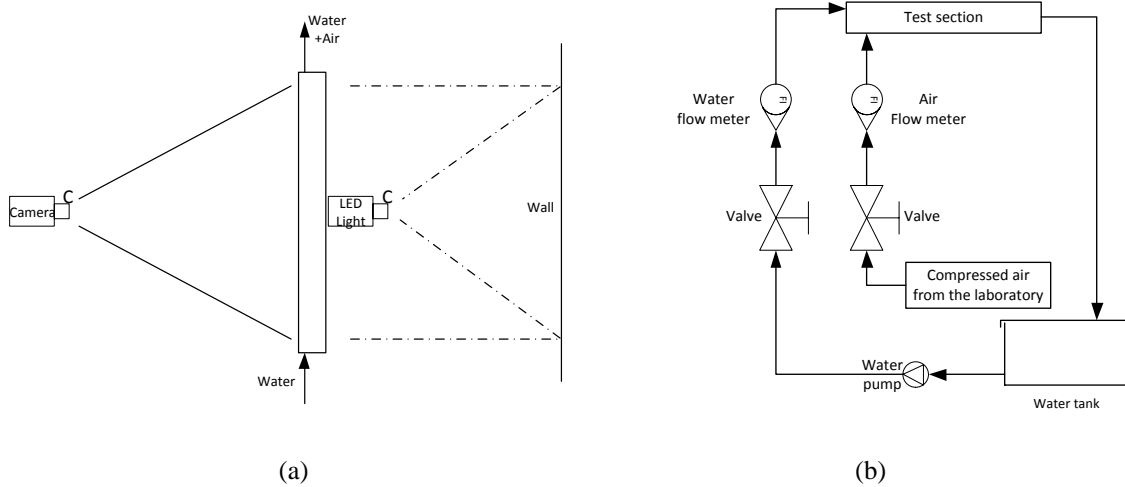


Figure 2: (a) The visualisation system setup, (b) Schematic of the test facility.

Figure 3 shows photos of two sheets of titanium felt and mesh, in which were taken using a mobile camera and a normal florescent light. Ti-felt has micro sized pores while the Ti-mesh has macro-sized holes. The Ti-felt has non-uniform pores distribution, while the Ti-mesh has uniform distributed holes. In this study, Ti-felt is used as a permeable wall.

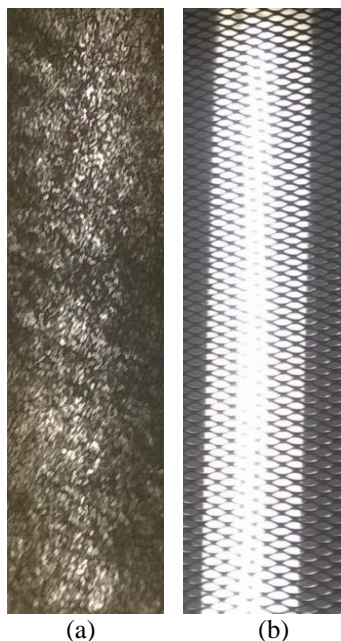


Figure 3: (a) Titanium felt, (b) Titanium mesh

Results and discussion

Flow pattern in vertical upward flow

Figure 4 shows grey scale images of the micro-channel for several water and air flow rates. (a) to (g) show images of the channel for a fixed flow rate of water 5.323 mL/min, while the air flow rate increased from 2.6 L/min to 31.2 L/min. As is shown, the air bubbles come out of the channel from specific points of the Ti-felt from top to bottom. In the other words, the structure does not generate a layer of bubbles that are evenly distributed along the length of the channel. As long as a single path offers the lowest pressure drop in the porous structure, air flows through this single rout and ignores the remaining cross-sectional area of the Ti-felt. By increasing the air flow rate, the pressure drop of the first rout increases. At a given pressure drop this then leads to another rout opening in the porous media to decrease the total air pressure drop. The growth of bubbles from specific points of the Ti-felt shows that the air flow in the saturated porous medium is highly capillary dominated, even at relatively high air flow rates found in high current density operation of electrolyzers.

The figure also reveals that a thin film of water separates the Taylor bubbles from each other.

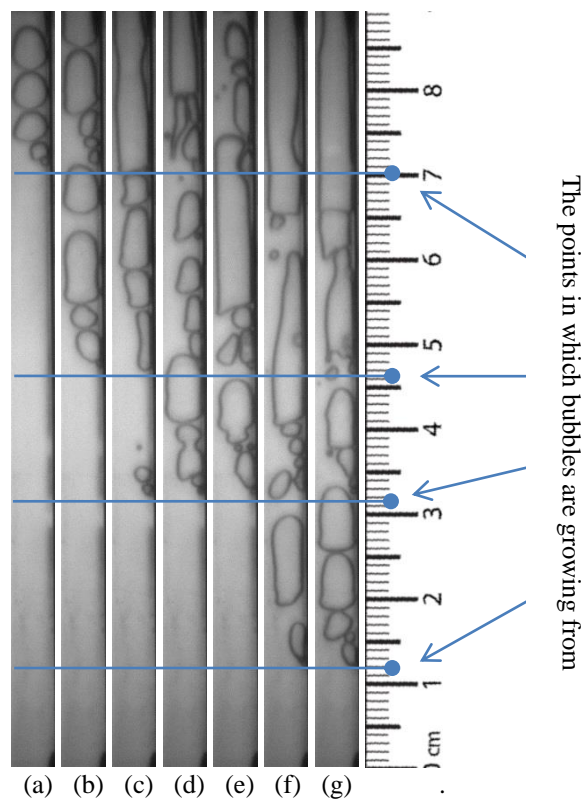


Figure 4: bubble growth from the permeable wall and movement in the micro-channel at different air flow rates, $Q_w = 5.323$ mL/min (mLPM), (a) $Q_a = 2.6$ LPM (L/min), (b) 5.2 LPM, (c) 10.4 LPM, (d) 15.6 LPM, (e) 20.8 LPM, (f) 26.0 LPM, (g) 31.2 LPM.

Figure 5 shows photos of the transparent channel in several air and water flow rates. The water flow rate doubled from (a) to (b) and the air flow rate also doubled from (b) to (c). Furthermore, to check reliability of the results, the air flow was made again by reducing from a high flow rate to the same as (c) to get the result of (d), which shows once penetration has been achieved the path will stay open.

As the bubbles come out of the Ti-felt, they move fast upward due to the influence of buoyancy. Small air bubbles merge together and form larger bubbles with the same depth as the channel and become surrounded by a thin layer of water. This effect decreases the bubble upward velocity due to an added mass effect (10). The upstream slugs with a smaller cross sectional area and higher upward speed eventually reach the bigger and slower downstream slugs and merge with them. Finally, the slugs get in touch with each other; this then creates an annular flow.

Yang et al. (8) have carried out similar work to this study in a $5 \times 5 \text{ mm}^2$ in cross-section area macro-channel with a block of porous lime wood as a permeable wall to get a uniform fine bubble generation at the surface of the porous media. They showed similar gas-liquid flow behaviour in their channel. The most significant difference to our study is seen in the number of moving bubbles in channel. In this study, due to the smaller cross sectional area, the number of the generated bubbles is very limited, while in the work by Yang et al. a great number of bubbles in the channel were observed.

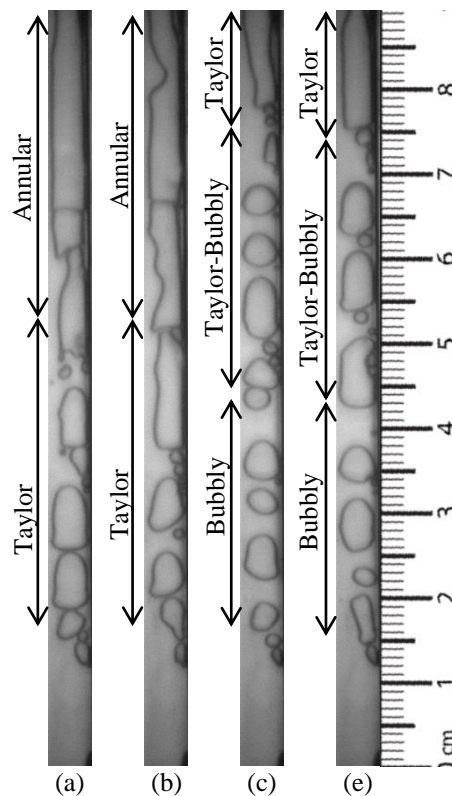


Figure 5: (a) $Q_w = 5.323 \text{ (mLPM)}$, $Q_a = 31.2 \text{ (LPM)}$, (b) $Q_w = 10.646 \text{ (mLPM)}$, $Q_a = 31.2 \text{ (LPM)}$, (c) $Q_w = 10.646 \text{ (mLPM)}$, $Q_a = 20.8 \text{ (LPM)}$, (d) $Q_w = 10.646 \text{ (mLPM)}$, $Q_a = 20.8 \text{ (LPM)}$.

Conclusion

The purpose of the study was to investigate the mechanism of growth of bubbles from the Titanium-felt and their behaviour in the micro-channel instead of studying an electrolysis cell which is subject to complex electrochemical phenomena that affects the control of the test parameters. Unfortunately, due to the non-uniform structure of Ti-felt pores, a uniform bubble growth from the surface was not seen. Instead, bubbles grew from specific points of the Ti-felt that had larger pores. Along the channel length coalescence of bubbles was observed. This meant that several gas-liquid flow regimes such as bubbly-Taylor flow, Taylor flow and annular flow regimes could be observed along the channel length.

To continue the research in this area and to improve the analysis, a layer of high flow resistant porous media with uniform nano-pores might be added. This presumed to result in growth of a more uniform layer of bubbles from the Ti-felt surface.

Acknowledgement

The authors would like to thank Saher A. Shakhshir for his kindly consultations in preparing the test setup.

References

1. K. Meier, *Int. J. Energy Environ. Eng.*, **5**, 2 (2014).
2. The Danish Ministry of Climate Energy and Building, (2012).
3. K. E. Ayers, E. B. Anderson, C. Capuano, B. Carter, L. Dalton, G. Hanlon, J. Manco, and M. Niedzwiecki, *ECS Transactions*, **33**, 1 (2010).
4. M. Carmo, D. L. Fritz, J. Mergel, and D. Stolten, *Int. J. Hydrogen Energy*, **38**, 12 (2013).
5. O. F. Selamet, U. Pasaogullari, D. Spornjak, D. S. Hussey, D. L. Jacobson, and M. D. Mat, *Int. J. Hydrogen Energy*, **38**, 14 (2013).
6. Dedigama, P. Angeli, K. Ayers, J. B. Robinson, P. R. Shearing, D. Tsaoulidis, and D. J. L. Brett, *Int. J. Hydrogen Energy*, **39**, 9 (2014).
7. Dedigama, P. Angeli, N. van Dijk, J. Millichamp, D. Tsaoulidis, P. R. Shearing, and D. J. L. Brett, *J. Power Sources*, **265**, (2014).
8. H. Yang, T. S. Zhao, and P. Cheng, *Int. J. Heat Mass Transf.*, **47**, 26 (2004).
9. H. Ito, T. Maeda, A. Nakano, A. Kato, and T. Yoshida, *Electrochim. Acta*, **100**, (2013).
10. M. Ishii, *Springer Science & Business Media*, (1975).